

Manuscript Number: JBB-D-13-01228R3

Title: Automated determination of poplar chip size distribution based on combined image and multivariate analyses

Article Type: Research Paper

Keywords: Cumulative size distribution curve; Sieving; Size classification; Biofuel quality determination; Modeling; Partial Least Squares

Corresponding Author: Dr. Corrado Costa, Ph.D.

Corresponding Author's Institution: Consiglio per la Ricerca e la sperimentazione in Agricoltura

First Author: Paolo Febbi

Order of Authors: Paolo Febbi; Paolo Menesatti, Ph.D.; Corrado Costa, Ph.D.; Luigi Pari, Ph.D.; Massimo Cecchini, Prof.

Abstract: The European technical standard EN 14961 on solid biofuels determines the fuel quality classes and specifications for wood chips. Sieving methods are currently used for the determination of particle size distribution. Some authors suggested that image analysis tools could provide methods for a more accurate measure of size integrated with shape. This work for the first time analyzes how image analysis combined with multivariate modeling methods could be used to construct cumulative size distribution curves based on chip mass (or weight). This has been done through a Partial Least Squares Regression model for the weight prediction of poplar chips and Partial Least Squares Discriminant Analysis models for estimation of chips size classification. Images of 7583 poplar chips were analyzed to extract size and shape descriptors (area, major and minor axis lengths, perimeter, eccentricity, equivalent diameter, fractal dimension index, Feret diameters and Fourier descriptors). The weight prediction model showed an high accuracy ($r = 0.94$). The chip classification based on three size fractions (8-16 mm, 16-45 mm and 45-63 mm), with or without Fourier descriptors, showed accuracies equal to 92.9% of correct classification for both models in the independent test. The combination of image analysis with multivariate modeling approaches allow a better conversion of image analysis results to sieve results using the esteemed weight. The proposed method will allow to standardize processes applicable by biofuels laboratories and machinery certifiers.

Response to Reviewers: Reviewers' comments:

Dear authors,

1) I have a different perception of fulfilling the requests for giving geo-coordinates of the growing and harvesting site and providing us the relevant information of the chain of custody of the poplar you used in your experiments. The information you have provided us so far is definitely insufficient to fulfill the standards of Biomass and Bioenergy.

Response to Reviewer's comment No. 1: We read some Biomass & Bioenergy papers trying to accomplish the reviewer request (B&B van Dam et al., 2008; B&B Facello et al., 2013). Following the scheme by Lewandowsky et al. (B&B 2006), we added the producer/forest (position and geo-coordinates), the processing plant/chipping machine, the transport information and the end use/experimental sieving. We hope that now these information (L107 to L114) will be adequate to fulfill the standards of Biomass & Bioenergy.

2) Moreover, I prefer to have intervals given as "figure1 to figure2" instead of "figure1 - figure2" as the latter could be interpreted also as a formulae which would result in a wrong interpretation. I leave this latter argument up to the decision of the editor in chief.

Response to Reviewer's comment No. 2: We are sorry but we did not find in the submitted MS the intervals "figure1 - figure2" to be substituted by "figure1 to figure2". We leave the editor to change this and other minor editing issues. However, we changed "root four- and stem two- years old: R4S2" into "root four-years and stem two-years old: R4S2" (L108)

Ms. Ref. No.: JBB-D-13-01228R2

Title: Automated determination of poplar chip size distribution based on combined image and multivariate analyses

Biomass and Bioenergy

Dear Dr. Corrado Costa,

The reviewers have commented on your above paper. They indicated that your paper is acceptable subject to the some minor revisions.

If you feel that you can suitably address the reviewers' comments (included below), I invite you to revise and resubmit your manuscript within 60 days.

Please carefully address the issues raised in the comments.

If you are submitting a revised manuscript, please also:

a) outline each change made (point by point) as raised in the reviewer comments

AND/OR

b) provide a suitable rebuttal to each reviewer comment not addressed

I look forward to receiving your revised manuscript.

Yours sincerely,

C.P. Mitchell

Editor

Biomass and Bioenergy

Dear Editor,

Please find attached our revised manuscript entitled “Automated determination of poplar chip size distribution based on combined image and multivariate analyses” (original MS# JBB-D-13-01228) to be considered for publication on Biomass and Bioenergy. We thank you and the referee for the time spent in reviewing our manuscript. We have now made the requested minor changes and carefully considered and addressed each specific point raised in order to improve its structure and better guide the reader. The list of our responses below shows how we have responded to the suggestions provided. We feel that these revisions have improved our paper and hope that now the paper could be accepted by your prestigious journal.

Best regards

Dr Corrado Costa (on behalf of all the authors)

Reviewers' comments:

Dear authors,

I have a different perception of fulfilling the requests for giving geo-coordinates of the growing and harvesting site and providing us the relevant information of the chain of custody of the poplar you used in your experiments. The information you have provided us so far is definitely insufficient to fulfill the standards of Biomass and Bioenergy.

Response to Reviewer's comment No. 1: We read some Biomass & Bioenergy papers trying to accomplish the reviewer request (B&B van Dam et al., 2008; B&B Facello et al., 2013). Following the scheme by Lewandowsky et al. (B&B 2006), we added the producer/forest (position and geo-coordinates), the processing plant/chipping machine, the transport information and the end use/experimental sieving. We hope that now these information (L107 to L114) will be adequate to fulfill the standards of Biomass & Bioenergy.

Moreover, I prefer to have intervals given as "figure1 to figure2" instead of "figure1 - figure2" as the latter could be interpreted also as a formulae which would result in a wrong interpretation. I leave this latter argument up to the decision of the editor in chief.

Response to Reviewer's comment No. 2: We are sorry but we did not find in the submitted MS the **intervals "figure1 - figure2"** to be substituted by **"figure1 to figure2"**. We leave the editor to change this and other minor editing issues. However, we changed "root four- and stem two- years old: R4S2" into "root four-years and stem two-years old: R4S2" (L108)

--> Accept subject to revisions

Kind regards

Walter Haslinger

Associate Editor

REVIEWER_ATTACH_DEEP_LINK_INSTRUCTIONS%

Highlights

Image analysis protocols were used to determine quality classes and dimensions of wood chips

2-D shape and size descriptors were extracted

PLS-R model was adopted to predict chips' weight

PLS-DA models were adopted to predict chips' size fraction

Cumulative size distribution curves based on predicted chip mass were constructed

1 **Automated determination of poplar chip size distribution based on combined image and**
2 **multivariate analyses**

3

4 Paolo Febbi^{1,2}, Paolo Menesatti¹, Corrado Costa^{1*}, Luigi Pari¹, Massimo Cecchini²

5

6 ¹ Consiglio per la Ricerca e la sperimentazione in Agricoltura - Unità di ricerca per l'ingegneria
7 agraria - Via della Pascolare 16, 00015 Monterotondo scalo (Rome), Italy.

8 ² Università della Tuscia - Dipartimento di Scienze e Tecnologie per l'Agricoltura le Foreste la
9 Natura e l'Energia- Via S. C. de Lellis s.n.c., 01100 Viterbo Italy.

10

11 * Corresponding author: Corrado Costa - Consiglio per la Ricerca e la sperimentazione in
12 Agricoltura - Unità di ricerca per l'ingegneria agraria - Via della Pascolare 16, 00015 Monterotondo
13 scalo (Rome), Italy - Phone +39-0690675214 - Fax +39-0690625591 - E-mail
14 corrado.costa@entecra.it

15

16 **Abstract**

17 The European technical standard EN 14961 on solid biofuels determines the fuel quality classes and
18 specifications for wood chips. Sieving methods are currently used for the determination of particle
19 size distribution. Some authors suggested that image analysis tools could provide methods for a
20 more accurate measure of size integrated with shape. This work for the first time analyzes how
21 image analysis combined with multivariate modeling methods could be used to construct
22 cumulative size distribution curves based on chip mass (or weight). This has been done through a
23 Partial Least Squares Regression model for the weight prediction of poplar chips and Partial Least
24 Squares Discriminant Analysis models for estimation of chips size classification. Images of 7583
25 poplar chips were analyzed to extract size and shape descriptors (area, major and minor axis
26 lengths, perimeter, eccentricity, equivalent diameter, fractal dimension index, Feret diameters and
27 Fourier descriptors). The weight prediction model showed an high accuracy ($r = 0.94$). The chip
28 classification based on three size fractions (8-16 mm, 16-45 mm and 45-63 mm), with or without
29 Fourier descriptors, showed accuracies equal to 92.9% of correct classification for both models in
30 the independent test. The combination of image analysis with multivariate modeling approaches
31 allow a better conversion of image analysis results to sieve results using the esteemed weight. The
32 proposed method will allow to standardize processes applicable by biofuels laboratories and
33 machinery certifiers.

34

35 **Keywords:** Cumulative size distribution curve; Sieving; Size classification; Biofuel quality
36 determination; Modeling; Partial Least Squares.

37

38 **Abbreviations**

39 C_{\min} = chip width measured by digital caliper

40 C_{\max} = chip length measured by digital caliper

41 D_{\min} = minimum Feret diameter

42 D_{\max} = maximum Feret diameter

43 FD = Fourier descriptor

44 LV = Latent Variable

45 P = designation for particle size distribution

46 PLS-DA = Partial Least Squares Discriminant Analysis

47 PLS-R = Partial Least Squares Regression

48 RMSEC = Root-Mean-Square Error of Calibration

49 RMSECV = Root-Mean-Square Error of Cross-Validation

50 RPD = Ratio of Percentage Deviation

51 SRF = Short Rotation Forestry

52 VIP = Variable Importance in the Projection

53

54 **1 Introduction**

55 The standard EN 14961-1:2010 determines the fuel quality classes and specifications for solid
56 biofuels [1]. The classification is based on the biofuel origin and source. Woody biomass is biomass
57 from trees, bushes and shrubs that may only have been subjected to size reduction, debarking,
58 drying or wetting. Solid biofuels are traded in many different sizes and shapes, which influence the
59 handling of the fuel as well as its combustion properties. Energy conversion and emissions are also
60 influenced by the particle sizes. In the case of wood chips, the properties of dimensions, moisture
61 and ash content are normative in the specification, whereas other properties (net calorific value,
62 bulk density, ash melting behavior) are informative. Particle size is important also during storage, as
63 it affects drying, calorific value and durability [2]. Together with moisture content, particle size
64 distribution defines the product quality.

65 The European technical standard EN 14961-4: 2011 [3] on solid biofuels determines the fuel quality
66 classes and specifications for non-industrial wood chips (used in smaller scale appliances, such as in
67 households and small commercial and public sector buildings). The sensitivity to the fuel quality
68 imposes a tighter specifications for small-size plants, whose small conveying ducts can be blocked
69 by oversize particles [4].

70 An oscillating screen method (using sieve apertures of 1 mm and above) is currently used for the
71 determination of particle size distribution, according to the standard EN 15149-1:2010 [5]. The
72 results of sieving are presented in cumulative size distribution curves: the cumulative percent mass
73 of each fraction with respect to the total mass of all fractions *versus* the particle size in mm. Size-
74 sorting by mechanical screening is used in many different industries, including conventional solid
75 fuels, such as coal. However, the screening of wood chips is not a generalized practice yet [4].

76 Particle form (*i.e.*, the combination of shape and size) influences if a particle passes a given sieve,
77 and the least cross sectional area is an important factor that has effect on the wood chips sieving
78 results. However, there are some disadvantages associated with sieve analysis, which is considered
79 a crude method of determining size [6] and not giving an exact measure of any dimension of the

80 particles. If a particle passes through a sieve is not only dependent upon its length and width but
81 also on thickness and shape; as the size difference between width and thickness increases, the
82 particle tends to pass through the sieve [7].

83 Image analysis could provide a method which is sensitive to the geometrical shape for determining
84 a more accurate measure of size integrated with shape [6]. Image analysis methods are generally
85 based on two-dimensional images of particle projection area and provide an accurate measure of
86 particle sizes. Typically, the result of this analysis is presented in size distribution curves, which are
87 not based on the cumulative percentage mass, as it is for sieve analysis, but refer to the percentage
88 of the total particle projection area (or particle number). Dynamic online image analysis systems are
89 considered particularly interesting because they can sort the particle sizes according to more than
90 just one size parameter [8]. Hartmann *et al.* [8] suggested it would be useful to launch a
91 standardization process in order to include the image analysis method to the scope of applicable
92 standard laboratory principles for biofuels, too, so as to overcome the drawbacks of the screening
93 methods. Following this suggestion, the aim of this study is to analyze how image analysis
94 combined with multivariate modeling methods can be used to construct cumulative size distribution
95 curves based on chip mass (or weight), which can be compared with the sieving results required by
96 EN standards. This has been done through a Partial Least Squares Regression (PLS-R) model for
97 the weight prediction of poplar chips and PLS Discriminant Analysis (PLS-DA) models for
98 estimation of chips size classification. A comparison between two PLS-DA models was conducted
99 to investigate the influence of the shape on the size fraction determination.

100

101 **2 Materials and Methods**

102 *2.1 Sample preparation*

103 Wood fuel chips consist of chipped woody biomass in the form of pieces with a defined particle
104 size produced by mechanical treatment with sharp tools, such as knives. Chips have a sub-

105 rectangular shape with a typical length of 5-100 mm and a low thickness compared to other
106 dimensions; wood chips in non-industrial situations have typical length of 5-50 mm [3].

107 The wood chips considered in this study came from the experimental harvesting of short-rotation
108 forestry (SRF) poplar (root four-years and stem two-years old: R4S2). The poplar plantation
109 (*Populus x canadensis*) was located in Musile di Piave (Venice, Italy; coordinates: 45°36'38.28" N;
110 12°31'14.46" E). Whole trees without roots were comminuted with a modified Claas Jaguar 890
111 machine using a rotor prototyped by CRA-ING [9]. Some samples were transported by van to
112 CRA-ING laboratory (Monterotondo, Rome, Italy). There, after air-drying, five 8-liter ($1\text{ l} = 1\text{ dm}^3$)
113 samples of poplar chips were sieved (oscillating screen method) for the determination of particle
114 size distribution, according to the standard EN 15149-1:2010 [5]. Sieves were used to separate the
115 wood chips in six dimensional classes: < 3.15 mm, 3.15-8 mm, 8-16 mm, 16-45 mm, 45-63 mm,
116 63-100 mm. The total weights of the particles between the sieve intervals were determined with a
117 precision scale and the result was expressed as a percentage of the total mass of all fractions. Then,
118 the wood chips were stored in the CRA-ING laboratory.

119 Wood chips may be delivered in specific trade classes, mostly on the basis of the main fraction
120 (minimum 75 weight-percentage): P16 (3.15-16 mm), P45 (8-45 mm), P63 (8-63 mm), P100 (16-
121 100 mm). The designation symbol for particle size distribution (P) is used in combination with a
122 number (P-class) for dimension referring to the particle sizes passing through the mentioned round
123 hole sieve size. The average numerical value from the whole lot (or defined portion from the lot)
124 determines the class to be used. The cross sectional area of the oversized particles shall be less than
125 a given value, in cm^2 (Tab. 1). *Gross* fraction identifies the particles quantity with dimensions
126 exceeding those reference values; *finer* fraction refers to the dimensions below the lower limit (<
127 3.15 mm).

128

129 [Insert Table 1 here]

130

131 The commercial classes P16, P45 and P63 describe high grade chips, suitable for the feeding of
132 small-size domestic (P16, P45) and residential boilers [10]. Generally, products with more uniform
133 sizes have been required.

134 While chips produced from logs always contain a smaller proportion of oversize particles and a
135 higher proportion of accepts (chips in the selected P-class) [2, 11], chips produced from tops,
136 branches and small stems tend to present a higher incidence of oversize particles [12]. For this
137 reason the analyzed chips were quite irregular in shape and size, and the sieved fractions were not
138 very uniform.

139

140 2.2 Chip size determination

141 The 7583 particles of the three wood chip size fractions (*i.e.*, dimensional classes; 8-16 mm, 16-45
142 mm, 45-63 mm) were divided in 2 sub-samples, by mass: a sub-sample corresponding to 12.5%
143 (1/8) of the mass of each fraction (706.4 g; 706 chips) and a sub-sample corresponding to remaining
144 mass (4946.9 g; 6877 chips). Each single chip in the first sub-sample (706 chips) was weighed, at
145 constant temperature and moisture content below 20 weight-percentage, with a resolution of 0.01 g;
146 then individual length (C_{\max}), width (C_{\min}) and thickness were measured with a resolution of 0.1
147 mm, using a digital caliper (Borletti CDJ 15). 100 chips were randomly selected for the
148 determination of moisture content (oven dry method, EN 14774-2:2009 [13]): the mean moisture
149 value, measured on the particles singularly, was 9.1 ± 0.8 %. The result was calculated to two
150 decimal places and rounded to the nearest 0.1 % for reporting.

151 The chip length was measured as the maximum expansion of the particle when oriented in a stable
152 position (longitudinal direction); the chip width was recorded as the second longest expansion
153 (perpendicular to the longitudinal direction), while the thickness was the third longest expansion
154 perpendicular to both length and width [8]. The particles were saved and numbered for future
155 analysis. Chips in the size fraction that passed the 8 mm sieve were not individually measured nor

156 further considered in the analysis. No wood chips in the 63-100 mm dimensional class were
157 obtained.

158 Digital images (Fig. 1a) of all chips in both sub-samples were acquired using a high resolution (600
159 dpi) digital scanner A3 Epson GT-10000+. The 2-D numerical data were processed in Matlab (rel.
160 7.1) environment. Images were segmented using the following procedure: *i.* a median filter (7x7)
161 was applied to each RGB channel, *ii.* for each pixel an Euclidean distance was calculated basing on
162 the RGB values and *iii.* a minimum error thresholding algorithm [14] was applied to binarize the
163 image.

164

165 [Insert Figure 1 here]

166

167 After image segmentation (Fig. 1b), the following 10 size descriptors were extracted from each
168 object: area, major and minor axis lengths, perimeter, eccentricity, equivalent diameter, fractal
169 dimension index [15], maximum, minimum and mean Feret diameters. Feret diameter is defined as
170 the distance between two parallel tangential lines restricting the object perpendicular to that
171 direction; it measures a particle size along a specified direction. The maximum and minimum Feret
172 diameters, D_{\max} and D_{\min} , are often used as the dimensions of the particles; they represent the
173 longest (*length*) and intermediate (*width*) dimensions of the particle projected area. Typically,
174 cumulative distribution curves of the size distribution based on image analysis use the actual lengths
175 of Feret diameters. Pixels were converted into metric scales through a scale factor (25.4/600).

176 Moreover, 99 Fourier coefficients were extracted; they summarize the shape of an object in the
177 frequency domain. Complex shapes can be represented with a small number of invariant
178 coefficients, which can be viewed as features extracted from the original shape boundaries [16].
179 Generally, a subset of the components of the Fourier descriptors (lower frequencies) is enough to
180 capture the overall features of the shape and to discriminate the different shapes [17].

181

182 2.3 Multivariate modeling

183 PLS-R is a particular type of multivariate analysis which uses a two-blocks predictive PLS model. It
184 relates the two data matrices (**X** and **Y**) by a linear multivariate model and models also the structure
185 of **X** (K column vectors: $\mathbf{x}_1, \dots, \mathbf{x}_K$) and **Y** (M column vectors: $\mathbf{y}_1, \dots, \mathbf{y}_M$); both these blocks are
186 assumed to be, at least partly, modeled by the same latent variables (not directly observed or
187 measured), LVs [18, 19]. The regression analysis objective is achieved by using the equation that
188 minimizes the residual mean square error, or maximizes the coefficient of multiple determination r^2 ,
189 which is the most commonly used statistic to measure the forecasting potential of a multiple
190 regression equation [20]. The predictive ability of the model depends also on the number of latent
191 vectors used. Because fit and prediction are different aspects of a model's performance, Root-
192 Mean-Square Error of Calibration (RMSEC) and Root-Mean-Square Error of Cross-Validation
193 (RMSECV) values for PLS were calculated as a function of the number of LVs in the model.
194 RMSEC is a measure of how well the model fits the data; RMSECV is a measure of a model's
195 ability to predict new samples that were not used to build the model. Generally, a good predictive
196 model should have high values of Pearson correlation coefficient (r), low values for RMSE and
197 maximum Ratio of Percentage Deviation (RPD). RPD is the ratio of the standard deviation of the
198 laboratory measured (reference) data to the RMSE of the cross-validation [21]. RPD values between
199 2.0 and 2.5 indicates very good, quantitative model and/or predictions; RPD values major than 2.5
200 indicates excellent model and/or predictions. [22].

201 PLS regression modeling was applied in order to estimate the weight of chips from size and shape
202 descriptors obtained by image analysis. The model adopted for weight prediction was selected from
203 540 PLS linear regression models considering the combination among **X** pre-processings (Abs,
204 Autoscale, Baseline, Detrend, Mean center, Median center, None, Normalize, Snv), **y** pre-
205 processings (Autoscale, Median center, None) and number of LVs, from 1 to 20 (the pre-processing
206 techniques are summarized in [23]). The PLS-R models were developed from a calibration set
207 (training/evaluation set [24]) of 530 chips (75% of the 706-chip sub-sample) with 109 X-variables

208 (10 size and 99 shape descriptors) and 1 y-variable (weight or mass). The PLS-R models (cross-
209 validated) were then validated on an internal test set of 176 chips (25% of the 706-chip sub-
210 sample). The partitioning were conducted optimally choosing the Euclidean distances based on the
211 algorithm of Kennard and Stone [25] that selects objects without the *a priori* knowledge of a
212 regression model. The PLS-R model selection was mainly based on the efficiencies and robustness
213 parameters described above. Once selected, the model was applied to the entire sample (7583
214 chips).

215 PLS-DA [26-28] is a PLS regression where the response variable is categorical, expressing the class
216 membership of the statistical units. The objective of PLS-DA is to find a model, developed from a
217 training set of observations of known class membership, that separates classes of objects on the
218 basis of their X-variables. The multistate and qualitative response variable, y, may be split into a set
219 of dummy variables (Y block) whose number is equal to the number of categories or classes. Its
220 modeling efficiency is the mean of sensitivity and specificity [29]. The sensitivity of the model is
221 given by the number of samples predicted as in the class divided by number actually in the class
222 (percent of true positive); the specificity is given, per each category, by the number of samples
223 predicted as not in the class divided by actual number not in the class (percent of true negative).

224 Some authors did not observe a direct correlation between the intermediate axis of the particle,
225 often defined as the ‘image analysis size’ of the particle, and sieve size; so, alternative methods
226 were investigated [7]. The determination of particle size distribution, as reported in the oscillating
227 screen method [5], provides a series of mutually exclusive size fractions (or classes) among which
228 the chips are included. This response variable (the particle class) was the classification criterion
229 used in discriminant analysis. PLS-DA was utilized as a supervised modeling method using
230 SIMPLS algorithm [30] to calculate a model for correlating image-analysis with sieving results.
231 Two different PLS-DA analyses were conducted. The first one considering 109 X-variables: 10 size
232 descriptors and 99 FDs; the second one considering only 10 explanatory variables, the same 10 size
233 descriptors, without the 99 FDs. The models adopted for the size fraction prediction of chips were

234 selected considering the combination between \mathbf{X} pre-processing (Abs, Autoscale, Baseline, Detrend,
 235 Diff1, gls weighting, Groupscales, Log1suR, Mean center, Median center, Msc (mean), None,
 236 Normalize, Snv) and the number of LVs (the pre-processing techniques are summarized in [23]).
 237 There was no \mathbf{Y} pre-processing. The models with FDs, using between 1 and 20 LVs, were 280; the
 238 models without FDs, using between 1 and 9 LVs, were 126. The chip membership to the three
 239 fractions was known before the analysis. The PLS-DA models were calibrated and validated on 100
 240 chips of fraction 8-16 mm, 100 chips of fraction 16-45 mm and 25 chips of fraction 45-63 mm; the
 241 225 particles were randomly extracted from the 706-chip sub-sample. This dataset was divided into
 242 a calibration set of 169 chips (75% of each group) and an internal validation set of 56 chips (25% of
 243 each group). This was done optimally choosing the Euclidean distances based on the algorithm of
 244 Kennard and Stone [25] that selects objects without the *a priori* knowledge of a regression model.
 245 The percentages of correct classification were calculated for calibration and validation phases, and
 246 then used for model selection, in both analyses (with and without FDs). The PLS-DA model
 247 selection was mainly based on the efficiencies and robustness parameters described above.
 248 In PLS-R and PLS-DA methods, a summary of the relative importance of the X -variables for both \mathbf{Y}
 249 and \mathbf{X} model parts is given by Variable Importance in the Projection (*VIP*) [31,32]. It is a weighted
 250 sum of squares of the PLS weights, taking into account the amount of explained Y -variance in each
 251 PLS component [33]. *VIP* has also the property of $\sum_{k=1}^K VIP_k^2 = K$, where K is the number of
 252 predictor variables [34]; the average of squared *VIP* scores equals 1. The explanatory variables with
 253 larger *VIP* values tend to be more important than others [32, 35], even if it does not mean that a
 254 variable with a low *VIP* is not relevant for the classification. In the case of PLS-DA, for each
 255 response variable, \mathbf{y}_m (m -th column vector of \mathbf{Y}), a regression model on the X -components was
 256 considered. For each k -th predictor variable, the VIP_k value quantifies the influence on the response
 257 of each variable summed over all components and categorical responses (for more than two
 258 categories in \mathbf{Y}) [34].

259 The VIP_k scores are a set of values equal in length to the number of X -variables included in the
260 model (K) and were calculated according to Chong *et al.* [36]. To summarize the contribution of all
261 the Fourier coefficients, a single summary variable was considered, whose value was calculated as
262 the root square of the sum of square of all 99 FDs scores.

263

264 **3 Results and discussion**

265 The determination of particle size distribution (standard EN 15149-1:2010 [5]) requires samples ($>$
266 $8l$; $1l = 1 \text{ dm}^3$) taken from stock or from deliveries (*e.g.* shipload, truckload) in accordance with the
267 sampling methods for solid biofuels (EN 14778:2011 [37]); methods for reducing combined
268 samples (or increments) to laboratory samples and laboratory samples to sub-samples and general
269 analysis samples are described in ‘Solid biofuels - Sample preparation’ (EN 14780:2011 [38]). In
270 addition, the standard requests to identify the particles over 100 mm, to specify their number and
271 size fraction, and to record the length of the longest particle overall. Image analysis accurately
272 measures several parameters allowing to satisfy these standard requirements. Generally, image
273 analysis is based on two-dimensional images of particles. Although the shape of the minimum
274 projected area of a particle theoretically influences how the particle passes the sieves [7], its
275 automated measurement is not easy to carry out and also the particle could be so long that it cannot
276 rotate and pass the screen holes vertically, even if it were thin enough to pass through.

277

278 *3.1 Typical cumulative distribution curves*

279 The manual measured *length* (C_{\max}) and *width* (C_{\min}), Feret diameters, D_{\max} and D_{\min} , and particle
280 weight (*i.e.*, observed) were used to construct the size-distribution curves with respect to the
281 cumulative percentage mass or to the cumulative percentage area (Fig. 2). The x -axis presents the
282 chip/hole size in mm.

283

284 [Insert Figure 2 here]

285

286 For data evaluation and statistical processing, the median value of the particles is considered being
287 less susceptible to outliers with respect to mean value [5, 8]. The median value is the observed
288 particle size of a sample that separates the cumulative size distribution into two equal parts (half of
289 the particle mass is below and half is above); graphically, it is given by the intersection point of the
290 cumulative size distribution curve with the 50%-horizontal line. The comparison among sieving,
291 image analysis and manual measurements showed a lateral relative displacement among the curves.
292 The curves relate the different sizes of the chips in the first sub-sample (706 chips). The further
293 apart the curves are, the more the difference among the axial dimensions of the chips. Observing the
294 median values, there is some compliance of the horizontal screening (sieve) result with the results
295 from image analysis method (D_{\min}).

296 Hartmann *et al.* [8] used a digital caliper as a reliable way of chip size determination and such
297 manual measurements were applied to build a reference distribution curve. Figure 2 shows that the
298 cumulative distribution curves based on C_{\min} and D_{\min} were very close each others. Even though
299 manual measurements of chip width (C_{\min}) are affected by errors and a slight tilting of the chip
300 position changes its projection area, and then its D_{\min} size, the linear correlation coefficient (Pearson
301 r) between D_{\min} and C_{\min} of the 706 chips was very high, 0.989. It is confirmed that image analysis
302 sizing could be considered a more accurate way of measuring chips with respect to the manual one,
303 due to human error and subjectivity associated with the manual measurements [39].

304

305 3.2 Weight (or mass) prediction

306 For the first time a cumulative distribution curve completely based on 2-D image analysis has been
307 constructed. The PLS-R model adopted for the weight prediction presents the characteristics and
308 principal results reported in Table 2. The selected model was not pre-processed. The estimated
309 number of LVs was 10; this number of significant components minimizes the residual errors for the
310 validation phase (RMSECV). The first two LVs, which capture most of the variance in \mathbf{X} -block

311 (99.97%) and **Y**-block (92.47%), have the maximum ability for the predictive model. The
312 cumulated variance of **X**-block was 100%, and the cumulated variance of **Y**-block was 95.1%. The
313 model correlation coefficient was 0.96, while the test correlation coefficient was 0.89; these values
314 are relatively high. The model RPD_{RMSE} value was 3.65, while test RPD_{RMSE} value was 2.16; these
315 values indicate an excellent/very good model [22]. The bias value was negligible ($< 10^{-3}$). The
316 loading values and VIP scores obtained by the PLS regression showed that area and perimeter
317 variables were truly significant for the model (data not shown).

318

319 [Insert Table 2 here]

320

321 Figure 3a shows the predicted weights *vs.* the observed weights of both 530 model and 176 test
322 chips; the Pearson r value between the observed and predicted weights of the 706 chips was 0.94.
323 The deviation between observed and predicted weight of chips was higher at higher weight values.
324 The predicted weight of the 706-chip sub-sample was 682.7 g, 96.6% of the observed weight. This
325 prediction model was developed using poplar chips at 9.1 ± 0.8 % moisture content. Using the same
326 chips, but with different moisture content, and adopting the same model, the predicted weight
327 values would remain the same, even if the measured weights were different; however, these
328 predicted values could be used for the subsequent construction of the cumulative size distribution
329 curve, because the cumulative particle share (%) is the same in both cases. Many existing methods
330 based their conversion of image-analysis size to sieve size on the intermediate axis [7]. Typically,
331 minimum Feret diameter (D_{min}) and manually weighted mass of each particle were used to construct
332 the cumulative distribution curves with respect to the cumulative percentage mass [7, 8]. Figure 3b
333 shows the size-distribution curves with respect to the cumulative percentage mass, where the ' D_{min}
334 predicted mass' distribution curve refers to the predicted mass. The cumulative distribution curve
335 completely based on 2-D image analysis is almost completely overlapping the cumulative
336 distribution curve constructed from the manually weighted mass of each chip.

337

338 [Insert Figure 3 here]

339

340 3.3 Chip size fraction prediction

341 The two selected PLS-DA models (with and without FDs) adopted for the size fraction prediction of
342 chips present the characteristics and principal results reported in Table 3. In both models, the **X** and
343 **Y** blocks were not pre-processed. The models were selected not only considering their
344 performances but hence considering their robustness (*sensu* [40]). The selected numbers of LVs, 12
345 and 9 respectively, minimized the respective RMSECV curves. The mean sensitivity and specificity
346 were always high: 94.7% and 93.1% for the model with FDs, 95.1% and 92% for the model without
347 FDs. Their efficiencies were 93.9% and 93.6%, respectively. The mean classification error was low
348 and equal to 6.1% for the model with FDs and 6.4% for the model without FDs. The mean
349 percentage of correct classification, calculated on 169 chips (training/evaluation set), was 92.3% for
350 the model with FDs and 92.9% for the model without FDs; the mean percentage of correct
351 classification for the internal test (56 particles) was 92.9% in both cases.

352

353 [Insert Table 3 here]

354

355 The discrimination ability is expressed through the percentage of well classified units. The random
356 probability to assign a generic chip to one of three fractions is 33%. Both PLS-DA models were
357 applied to all 7583 wood chips (external test) to evaluate their ability to assign the chip size fraction
358 more accurately than what would occur by chance. The classification results (confusion matrices)
359 are reported in Table 4. The mean percentage of correct classification for the external test was
360 89.6% for the model with FDs and 89.2% for the model without FDs. The efficiencies of both
361 models were slightly higher than 88%.

362

363 [Insert Table 4 here]

364

365 The VIP scores of both models (12 LVs with FDs and 9 LVs without FDs) are reported in Figure 4.
366 Figure 4a shows the VIP_k parameters *per* each fraction of the model with Fourier descriptors, where
367 the FDs variable summarizes the overall contribution of all the Fourier coefficients. All the VIP_k
368 scores were higher than 1, demonstrating that all the explanatory variables were important for
369 explaining the prediction variables. Area variable had the higher VIP scores, therefore it was the
370 most significant variable in comparing the difference among the three size fractions. Figure 4b
371 shows the VIP_k parameters *per* each fraction of the model without Fourier descriptors. The VIP_k
372 scores expressed a relative weight of the explanatory variables: area, equivalent diameter and mean
373 Feret diameter were more important predictors in comparing the difference among the three
374 considered fractions; eccentricity and fractal dimension index did not seem to be significant.

375

376 [Insert Figure 4 here]

377

378 Even if the model with FDs is slightly more performing, there are not significant differences
379 between the two models, when a round hole sieve is used for determination of particle size
380 distribution. Some papers [6, 41] state that area, perimeter and Feret diameters are able to
381 mathematically distinguish and differentiate the particle shapes. The obtained results demonstrated
382 that multivariate analyses are able to technically realize, in a multidimensional space, this shape
383 distinction and to discriminate among classes, even if FDs are more informative.

384

385 3.4 Sieving software simulation

386 While traditional image analysis constructs size distribution curves with respect to cumulative
387 percentage area or percentage number of particles [6, 8], sieve analysis is typically presented in
388 percentage cumulative weight [5]. In order to use image analysis and construct size distribution

389 curves based on cumulative percentage mass, some researchers [42-46] used the determination of
390 the volume of a particle to calculate its mass. The results of these methods were considered not
391 perfectly accurate [7].

392 Image and multivariate analyses recognize shapes and relate these results to sieve size. Considering
393 the size fraction assignment obtained by the two PLS-DA models and the weight predicted by the
394 PLS-R model to each particle of the entire sample (7583 wood chips), a conversion from image-
395 analysis morphometries to sieving result was realized. This conversion depended upon an
396 appropriate estimate of the chip weights, even if an exact determination of mass is not necessary for
397 constructing the size distribution curve [7]. In fact, the cumulative size distribution curve refers to
398 the weight-percentage and is, for this reason, independent of the wood density (*i.e.*, wood species)
399 or the moisture content, when the moisture value is the same for all the chips. In the graph of
400 cumulative size distribution, even if the observed chip weights change, the cumulative particle share
401 (%) remains the same. This study was conducted on poplar wood chips, but the principles could be
402 extended, as demonstrated, to other wood species or different, but homogeneous (*i.e.*, low standard
403 deviation), moisture contents. In the specific case, the predicted weight of the entire three-fraction
404 sample (7583 chips) was 5539.3 g, 98% of the observed weight. The cumulative size distribution
405 curves completely based on image analysis are reported in Figure 5, as result of 706-chip and 7583-
406 chip tests. The cumulative curves of the two models were almost completely overlapping and very
407 close to the traditional curve based on sieve analysis. They give a good quantification of particle
408 size distribution. The advantage of image and multivariate analyses is to construct cumulative
409 distribution curves showing a good agreement with the sieve results and without the need of manual
410 measurements, generally time consuming. Since the proposed method, based on image analysis, and
411 the traditional sieving method can now produce the same type of curve, a direct comparison of their
412 results becomes easier.

413

414 **4 Conclusions**

415 The proposed method could be implemented on an online detection machine for particle size
416 characterization, revealing particularly helpful when the P-class to be specified (the number of
417 property levels) shall be determined from large quantities (the whole lot) or when frequent sampling
418 is required (*e.g.*, for an internal quality system). More samples or large amounts would reduce the
419 uncertainty arising from sampling and potentially could increase the quality and value of wood
420 chips.

421 The detailed information of chip form and other dimensional aspects provided by the method
422 proposed in this work could help: *i.* quality managers of large biofuel suppliers or purchasers to
423 check the fulfillment of particle size demands of the quality classes given in the standards, *ii.*
424 chipper machine constructors to verify the prototype performances depending from different
425 settings (knives position and number, cutting and feeding speeds, cutting and sharpness angles,
426 anvil height, cutting direction, etc.) in a given experimental situation, not easily related to sieve size,
427 and to optimize parameters of comminution devices in engineering situation, and *iii.* engineering
428 machine certification in order to fix standard methodologies highly replicable. An improvement of
429 the results is expected introducing a thickness measure. A 3-D analysis could prove to be
430 significant.

431

432 **Acknowledgments**

433 The authors would like to thank Angelo Del Giudice for the provision of sieved wood chips, and
434 Andrea Acampora for his help in manual measurements.

435

436 **References**

- 437 [1] EN 14961-1:2010. Solid biofuels - Fuel specifications and classes - Part 1: General
438 requirements, CEN European Committee for Standardization.
- 439 [2] Nati C, Spinelli R, Fabbri P. Wood chips size distribution in relation to blade wear and screen
440 use. Biomass Bioenerg 2010;34(5): 583–7.

441 [3] EN 14961-4: 2011. Solid biofuels - Fuel specifications and classes - Part 4: Wood chips for non-
 442 industrial use, CEN European Committee for Standardization.

443 [4] Spinelli R, Ivorra L, Magagnotti N, Picchi G. Performance of a mobile mechanical screen to
 444 improve the commercial quality of wood chips for energy. *Bioresour Technol* 2011;102(15): 7366–
 445 70.

446 [5] EN 15149-1:2010. Solid biofuels – Determination of particle size distribution – Part 1:
 447 oscillating screen method using sieve apertures of 1 mm and above, CEN European Committee for
 448 Standardization.

449 [6] Fernlund JMR. The effect of particle form on sieve analysis: a test by image analysis. *Eng Geol*
 450 1998;50(1): 111–24.

451 [7] Fernlund JMR, Zimmerman RW, Kragic D. Influence of volume/mass on grain-size curves and
 452 conversion of image-analysis size to sieve size. *Eng Geol* 2007;90(3): 124–37.

453 [8] Hartmann H. Methods for size classification of wood chips. *Biomass Bioenerg* 2006;30(11):
 454 944–53.

455 [9] Pari L, Civitarese V, Del Giudice A. Quality of wooden chips produced by CLAAS Jaguar
 456 equipped with experimental CRA-ING rotor. In: *Proceedings of the 18th European Biomass*
 457 *Conference and Exhibition. From research to industry and markets, Lyon, France 3-7 May 2010:*
 458 1717–20.

459 [10] Garstang J, Weekes A, Poulter R, Bartlett D. Identification and characterization of factors
 460 affecting losses in the large-scale, non ventilated bulk storage of wood chips and development of
 461 best storage practices. London: First Renewables Ltd, for DTI. p. 119; 2002.

462 [11] Assirelli A, Civitarese V, Fanigliulo R, Pari, L, Pochi D, Santangelo E, *et al.* Effect of piece
 463 size and tree part on chipper performance. *Biomass Bioenerg* 2013;54: 77–82.

464 [12] Manzone M, Spinelli R. Wood chipping performance of a modified forager. *Biomass Bioenerg*
 465 2013;55: 101–6.

466 [13] EN 14774-2:2009. Solid biofuels – Determination of moisture content – Oven dry method –
 467 Part 2: Total moisture – Simplified method. CEN European Committee for Standardization.

468 [14] Kittler J, Illingworth J. Minimum error thresholding. *Pattern Recognit* 1986;19(1): 41–7.

469 [15] Matabos M, Aguzzi J, Robert K, Costa C, Menesatti P, Company JB, *et al.* Multi-parametric
 470 study of behavioural modulation in demersal decapods at the VENUS cabled observatory in
 471 Saanich Inlet, British Columbia, Canada. *J Exp Mar Biol Ecol* 2011;401(1): 89–96.

472 [16] Aguzzi J, Costa C, Fujiwara Y, Iwase R, Ramirez-Llorda E, Menesatti P. A novel
 473 morphometry-based protocol of automated video-image analysis for species recognition and activity
 474 rhythms monitoring in deep-sea fauna. *Sensors* 2009;9(11): 8438–55.

475 [17] Zhang D Lu G. A Comparative Study of Fourier Descriptors for Shape Representation and
 476 Retrieval, In: *Proceedings of the 5th Asian Conference of Computer Vision (ACCV '02)* Jan. 2002:
 477 646–51.

478 [18] Wold S. PLS-Regression: a Basic Tool of Chemometrics. *Chemometrics Intell Lab*
 479 *Syst*2001;58(2): 109–30.

480 [19] Costa C, Menesatti P, Spinelli R. Performance modelling in forest operations through partial
 481 least square regression. *Silva Fenn* 2012;46(2): 241–52.

482 [20] Legendre P, Legendre L. *Numerical ecology*. 2nd English ed. Amsterdam: Elsevier; 1998.

483 [21] Williams PC. Variables affecting near-infrared reflectance spectroscopic analysis. In: Williams
 484 P, Norris K, editors. *Near-Infrared Technology in the Agricultural and Food Industries*, St Paul,
 485 Minnesota: American Association of Cereal Chemists; 1987: p. 143–66.

486 [22] Viscarra Rossel RA, Taylor HJ, McBratney AB. Multivariate calibration of hyperspectral
 487 gamma-ray energy spectra for proximal soil sensing. *Eur J Soil Sci* 2007; 58(1): 343–53.

488 [23] Antonucci F, Menesatti P, Holden NM, Canali E, Giorgi S, Maienza A, *et al.* Hyperspectral
 489 visible and near-infrared determination of copper concentration in agricultural polluted soils.
 490 *Commun Soil Sci Plant Anal* 2012;43(10): 1401–11.

- 491 [24] Forina M, Oliveri P, Lanteri S, Casale M. Class-modeling techniques, classic and new, for old
492 and new problems. *Chemometr Intell Lab Syst* 2008;93(2): 132–48.
- 493 [25] Kennard RW, Stone LA. Computer aided design of experiments. *Technometrics* 1969;11(1):
494 137–48.
- 495 [26] Sjöström M, Wold S, Söderström B. PLS discrimination plots. In: Gelsema ES, Kanals LN,
496 editors. *Pattern recognition in practice II*, Amsterdam: Elsevier; 1986.
- 497 [27] Sabatier R, Vivein M, Amenta P. Two approaches for discriminant partial least square. In:
498 Schader M, Gaul W, Vichi M, editors. *Between data science and applied data analysis*, Berlin:
499 Springer-Verlag; 2003.
- 500 [28] Costa C, Antonucci F, Boglione C, Menesatti P, Vandeputte M, Chatain B. Automated sorting
501 for size, sex and skeletal anomalies of cultured seabass using external shape analysis. *Aquacult Eng*
502 2013;52: 58–64.
- 503 [29] Derde MP, Massart DL. UNEQ: a disjoint modelling technique for pattern recognition based
504 on normal distribution. *Anal Chim Acta* 1986;184: 33–51.
- 505 [30] de Jong S. SIMPLS: an alternative approach to partial least squares regression. *Chemometr*
506 *Intell Lab Syst* 1993;18(3): 251–63.
- 507 [31] Wold S, Ruhe A, Wold H, Dunn WJ. III. The collinearity problem in linear regression. The
508 partial least squares approach to generalized inverses. *Siam J Sci Stat Comput* 1984;5(3): 735–43.
- 509 [32] Taiti C, Costa C, Menesatti P, Comparini D, Bazihizina N, Azzarello E, *et al.* Class-modeling
510 approach to PTR-TOFMS data: a peppers case study. *J Sci Food Agricult* 2014 (in press) DOI:
511 10.1002/jsfa.6761
- 512 [33] Peolsson A, Peolsson M. Predictive factors for long-term outcome of anterior cervical
513 decompression and fusion: a multivariate data analysis. *Eur Spine J Mar* 2008;17(3): 406–14.
- 514 [34] Perez-Enciso M, Tenenhaus M. Prediction of clinical outcome with microarray data: a partial
515 least squares discriminant analysis (PLS-DA) approach. *Hum Genet* 2003;112(5-6): 581–92.

516 [35] Zhang QZ, Zhang RC, Liu MQ. A method for screening active effects in supersaturated
517 designs. *J Statist Plann Inference* 2007;137(6): 2068–79.

518 [36] Chong IG, Jun CH. Performance of some variable selection methods when multicollinearity is
519 present. *Chemometr Intell Lab Syst* 2005;78(1): 103–12.

520 [37] EN 14778:2011. Solid biofuels – Sampling. CEN European Committee for Standardization.

521 [38] EN 14780:2011. Solid biofuels – Sample preparation. CEN European Committee for
522 Standardization.

523 [39] Fernlund JMR. Image analysis method for determining 3-D size distribution of coarse
524 aggregates. *Bull Eng Geol Env* 2005;64(2): 159–66.

525 [40] Swierenga H, de Groot PJ, de Weijer AP, Derksen MWJ, Buydens LMC. Improvement of PLS
526 model transferability by robust wavelength selection. *Chemometr Intell Lab Syst* 1998;41(2): 237–
527 48.

528 [41] Febbi P, Costa C, Menesatti P, Pari L. Determining wood chip size: image analysis and
529 clustering methods. *J Agricult Eng* 2013;44(s1): 519–21.

530 [42] Mora CF, Kwan AKH. Sphericity, shape factor, and convexity measurement of coarse
531 aggregate for concrete using digital image processing. *Cem Concr Res* 2000;30(3): 351–8.

532 [43] Rao C, Tutumluer E, Stefanski JA. Coarse aggregate shape and size properties using a new
533 image analyzer. *J Test Eval* 2001;29(5): 79–89.

534 [44] Maerz NH. Technical and computational aspects of the measurement of aggregate shape by
535 digital image analysis. *J Comput Civil Eng* 2004;18(1): 10–8.

536 [45] Taylor MA. Using multiple 3-D projections to characterize 3-D irregular particles. 12th Annual
537 Symposium of the International Center for Aggregate Research (ICAR) 2004; Austin. Texas.

538 [46] Tutumluer E, Pan T, Carpenter SH. Investigation of aggregate shape effects on hot mix
539 performance using an image analysis approach. *Civil Engineering Studies. Transportation*
540 *Engineering Series 137* University Illinois, Urbana-Champaign, 122 pp.; 2005.

Figure captions

Figure 1: Wood chips; original scanned image (a) and image after segmentation (*i.e.*, binarization) (b)

Figure 2: Cumulative distribution curves for different testing methods applied on the 706 poplar chips, referring to the chip mass (a) and area (b).

Notes: Sieve refers to sieving; Cmin and Cmax are the chip width and length measured by digital caliper; Dmin and Dmax are the minimum and maximum Feret diameters.

Figure 3: Comparison between the observed weight (or mass) and the predicted one using the Partial Least Squares Regression model (a). Comparison between cumulative distribution curves applied on the 706-chip sub-sample, referring to observed and predicted mass (b).

Notes: Sieve refers to sieving; Dmin is the minimum Feret diameter.

Figure 4: Partial Least Squares Discriminant Analysis models for size fraction prediction. VIP (Variable Importance in the Projection) scores of X-variables for the three size fractions (8-16, 16-45, 45-63), with Fourier descriptors in contracted form (*i.e.*, root square of the sum of square of all 99 FDs scores) for the 12 LVs model (a) and without Fourier descriptors for the 9 LVs model (b). The y axes have different magnitude because refer to two different models, and the VIP scores express the relative importance of the X-variables within each model.

Figure 5: Comparison among cumulative distribution curves determined by horizontal sieving (sieve - observed) and image analysis coupled with the Partial Least Squares Discriminant Analysis

models, with (12LVs with FDs) and without Fourier descriptors (9LVs without FDs), applied on the 706-chip (a) and 7583-chip (b) samples.

Tables

Table 1: Dimensions for wood chips (EN 14961-1:2010) considered in this work.

Particle size distribution	Main fraction, mm (min. 75 w-%)	Cross sectional area, cm ²	Coarse fraction, max length of particle, mm
P16	3.15-16	< 1	< 31.5/120
P45	8-45	< 5	< 120/350
P63	8-63	< 10	< 350
P100	16-100	< 18	< 350

Table 2: Characteristics and principal results of the Partial Least Squares Regression model to estimate the chips' weight (or mass).

Number of particles	530
n° LVs	10
% Cumulated variance X -block	100
% Cumulated variance Y -block	95.14
RMSEC	0.1937
RMSECV	0.2020
Bias	- 0.00067
<i>r</i> model	0.96
<i>r</i> test	0.89
RPD _{RMSE} model	3.65
RPD _{RMSE} test	2.16
LVs = Latent Vectors; RMSEC = Root-Mean-Square Error of Calibration; RMSECV = Root-Mean-Square Error of Cross-Validation; RPD = Ratio of Percentage Deviation.	

Table 3: Characteristics and principal results of the selected PLS-DA models, with Fourier descriptors (FDs) and without Fourier descriptors (no FD), to predict the three size fractions (8-16, 16-45, 45-63).

PLS-DA model	FDs	no FD
Number of particles	169	
n° size fractions (Y -block)	3	
n° LVs	12	9
X pre-processing	None	
% Cumulated variance X -block	100	100
% Cumulated variance Y -block	82.2	80.3
Mean sensitivity, %	94.7	95.1
Mean specificity, %	93.1	92
Efficiency	93.9	93.6
Random probability, %	33.3	
Mean classification error, %	6.1	6.4
Mean RMSEC	0.2382	0.2501
Mean % correct classification model	92.3	92.8
Mean % correct classification test	92.9	92.9
Mean % correct classification external test	89.6	89.2
PLS-DA = Partial Least Squares Discriminant Analysis; LVs = Latent Vectors; RMSEC = Root-Mean-Square Error of Calibration.		

Table 4: Confusion matrices of the 7583-chip external test (3 classes/fractions: 8-16, 16-45, 45-63) obtained from the two Partial Least Squares Discriminant Analysis models with and without Fourier descriptors (FDs)

Predicted (with FDs)				
Observed	Fraction 8-16	Fraction 16-45	Fraction 45-63	Total
Fraction 8-16	4838	106	11	4955
Fraction 16-45	641	1936	26	2603
Fraction 45-63	0	8	17	25
Predicted (no FD)				
Observed	Fraction 8-16	Fraction 16-45	Fraction 45-63	Total
Fraction 8-16	4854	96	5	4955
Fraction 16-45	687	1890	26	2603
Fraction 45-63	0	8	17	25

Figure 1
[Click here to download high resolution image](#)

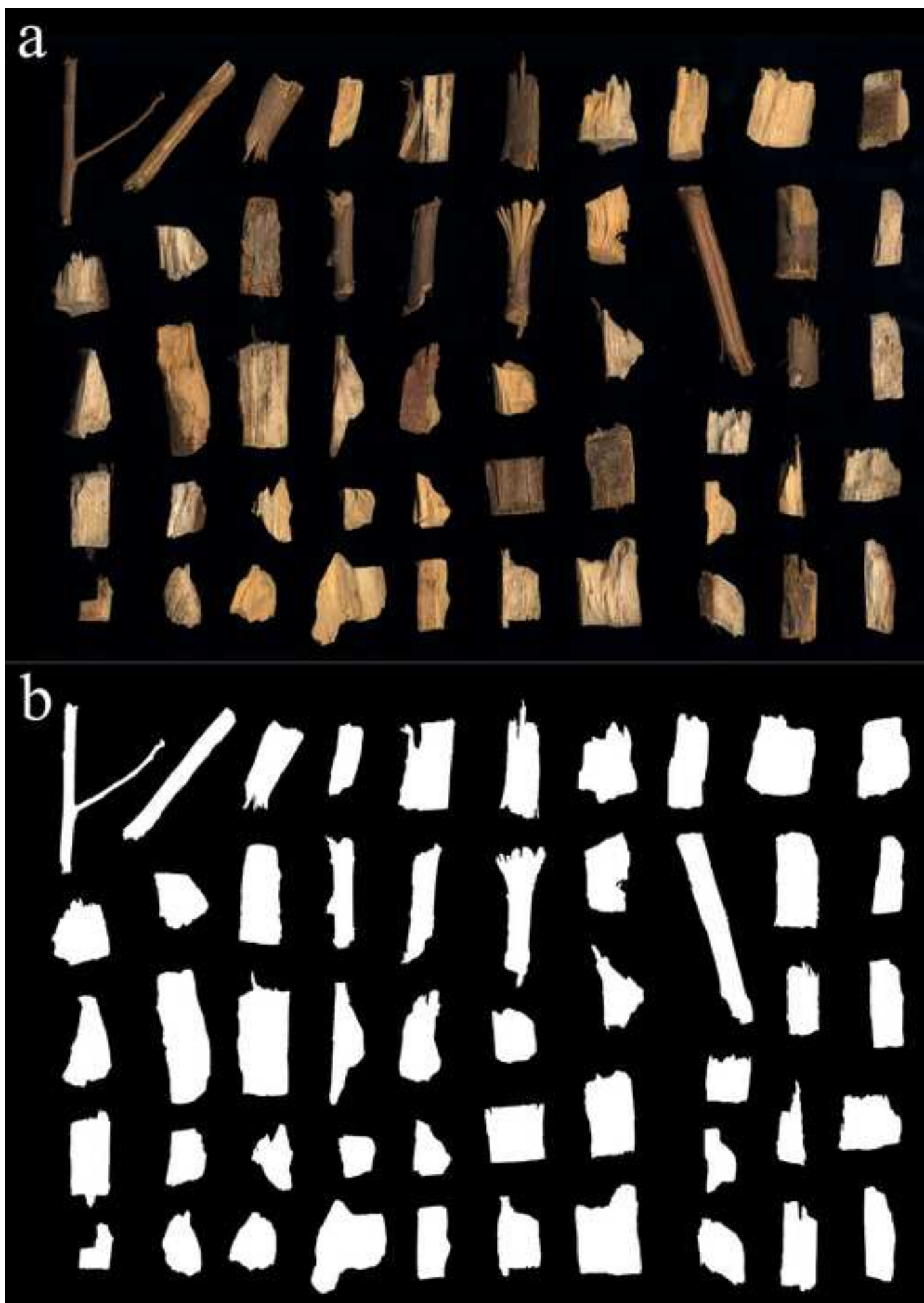


Figure 2
[Click here to download high resolution image](#)

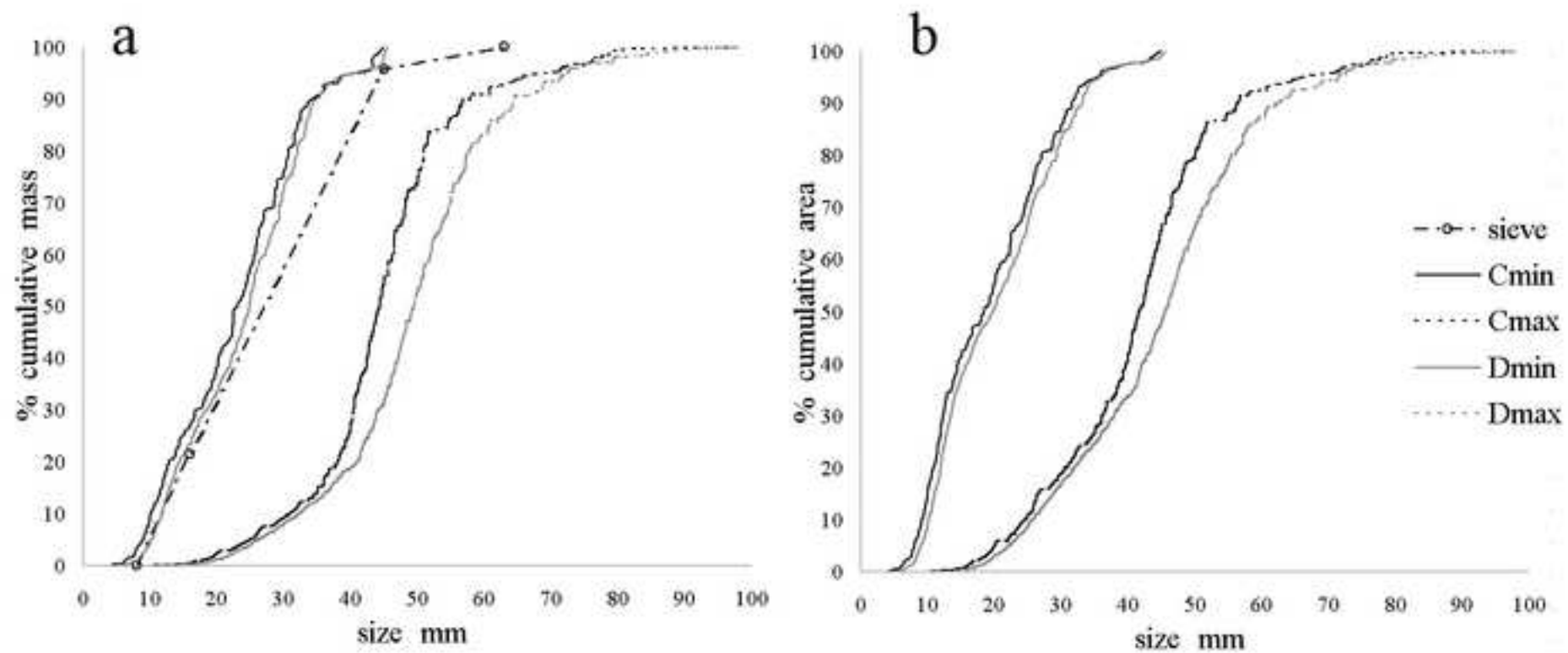


Figure 3
[Click here to download high resolution image](#)

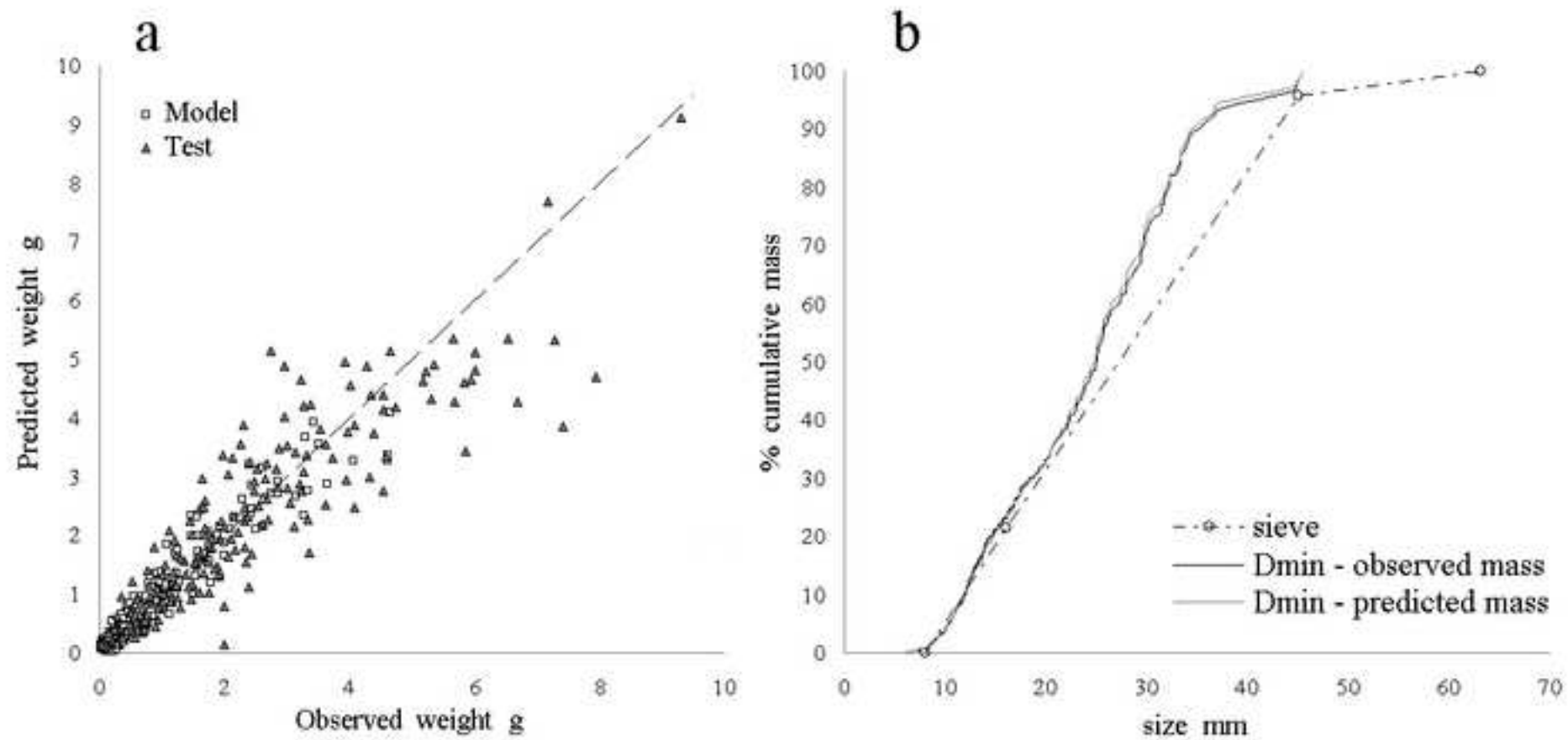


Figure 4
[Click here to download high resolution image](#)

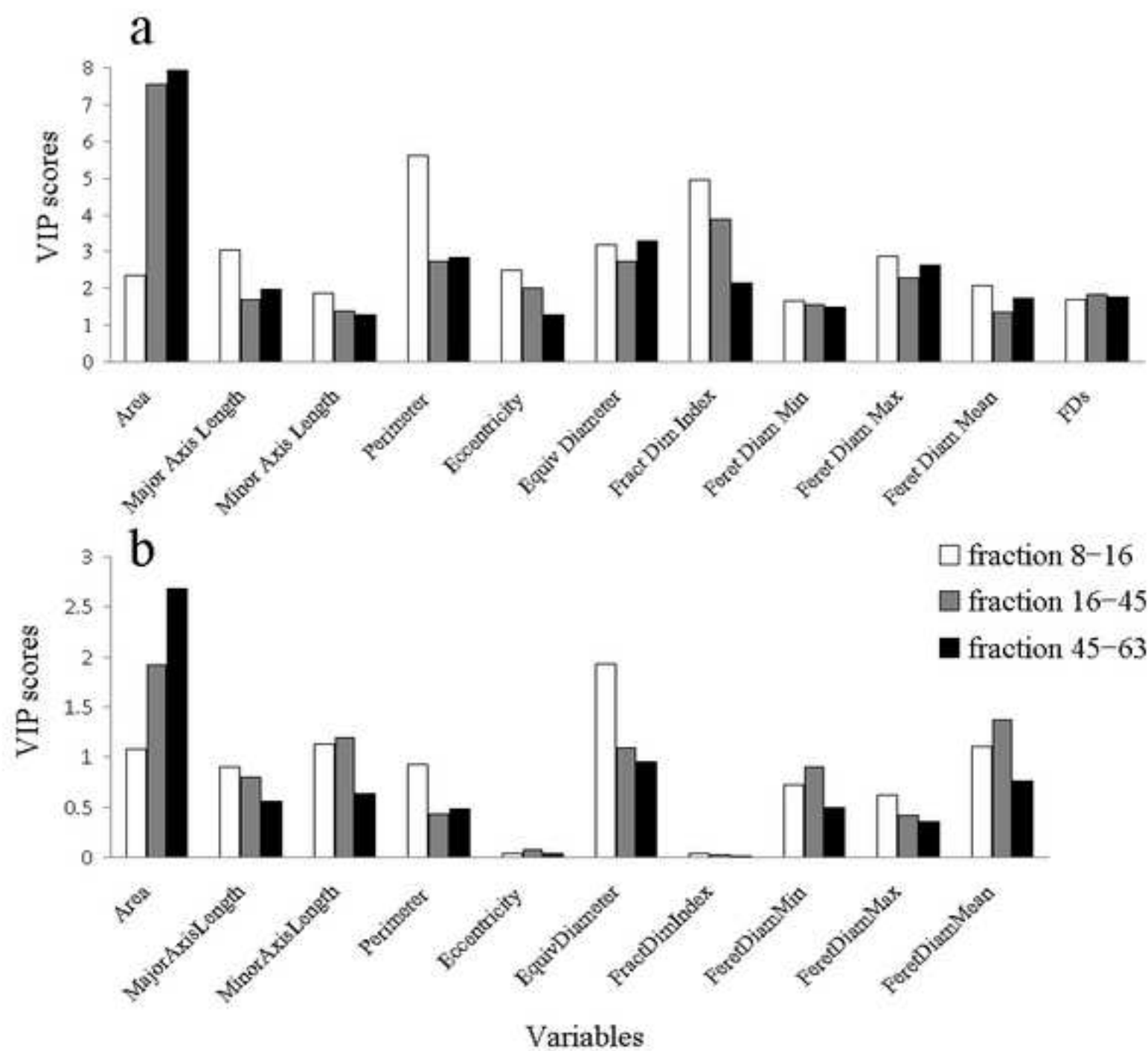


Figure 5
[Click here to download high resolution image](#)

